JOURNAL OF MATERIALS SCIENCE 24 (1989) 471–476

Electron transport in selenium-based amorphous xerographic photoreceptors

S. M. VAEZI-NEJAD
Electronic Research Group, School of Engineering, Thames Polytechnic, Wellington Street, London SE18 8PF, UK

C. JUHASZ
Solid State Group, Department of Electrical Engineering, Imperial College of Science and Technology, University of London, Exhibition Road, London SW7 2BT, UK

The present paper is the sequel to a previous report. In this paper, electron transport in various selenium-based amorphous xerographic photoreceptors is described. As before, measurements were carried out using xerographic time-of-flight (XTOF) and conventional time-of-flight (TOF) experiments. From the observed flight time the electron drift mobility μ_e was deduced. Transient photocurrent signals were also recorded at low fields to determine the decay time constant. For a given composition, the sample thickness, light intensity, substrate material and top contacts (in TOF) were varied to investigate whether the observed decay time constant τ_e is a meaningful bulk parameter as in the case of hole transport. Detailed results will be presented to show that the interpretation of τ_e is complicated. The more plausible explanation for the observed decay is the presence of a uniform distribution of positive space charge in the bulk. μ_e and τ_e were also measured as a function of composition and applied field. Experimental data suggest that electron transport is shallow trap-controlled. Light doping of selenium with arsenic or tellurium creates shallow traps and hence reduced μ_e. The field dependence of electron mobility is in the form $\mu_e \propto E^n$ where E is the applied field and n is a constant less than unity. No electron response can be detected in chlorine-doped Se–As or Se–Te alloys.

1. Introduction

In a recent paper hole transport in various amorphous selenium-based photoreceptors was discussed [1]. In this paper we present the results of experimental investigations of electron transport. As before, both conventional time-of-flight (TOF) and xerographic time-of-flight (XTOF) experiments were carried out under small-signal conditions [2, 3]. Samples were fabricated by vacuum evaporation and characterized as described before [1].

2. Transport measurements

2.1. Pure selenium

Both XTOF and TOF transient current signals exhibited features sensitive to the applied field. With t_T denoting the transit time, the features were

(i) An initial spike at $t \ll t_T$ which scales with the field and disappears at high fields;

(ii) a relatively slower decay following the spike at $t < t_T$; and

(iii) a slowly decaying tail which also scales with the applied field at $t > t_T$.

Fig. 1 shows typical transient signals recorded at different applied fields. Note that the deviation from single-exponential behaviour is very noticeable at a lower field. If the time constant of the initial decay is denoted by τ_s and the decay of the rest of the signal prior to t_T is denoted by τ_e, the experimental results clearly show that both these time constants are field-dependent. As shown on the log–log plots in Fig. 2, τ_e in both experiments decreases with field and the form of the field dependency is somewhat different among the samples. Apart from the initial and final portions of these curves. It is possible to represent the data by straight lines indicating

$$\tau_e \propto E^{-k} \quad (1)$$

where k is a constant less than unity. In order to examine the effect of contacts, TOF experiments were carried out on identical samples with gold, aluminium and copper as top contacts. Transient signals for the same applied voltage are shown in Fig. 3. The semilogarithmic plots of log $I(t)$ against t for these signals are shown in Fig. 4. τ_e estimated from the slopes of these lines is 40 to 47 μsec, depending on the top contact. From plots similar to these, values of τ_e for different applied fields were calculated. Fig. 5 shows the field dependence of τ_e for the waveforms in Fig. 3. It is evident that τ_e can be expressed by Equation 1 over a wide range of fields and the value of k for gold, aluminium and copper as top electrodes are 0.7, 0.9 and 0.8, respectively. For gold and copper, the τ_e values are very similar and smaller than the

0022–2461/89 $03.00 + .12

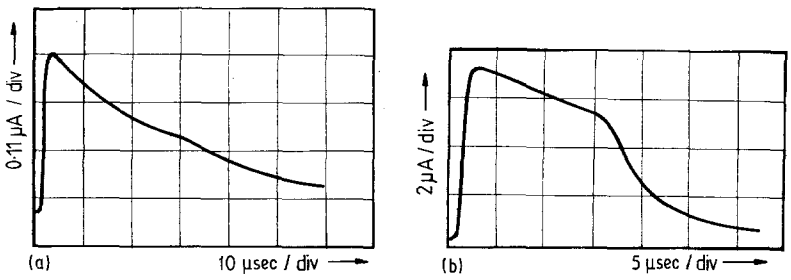

Figure 1 Typical XTOF and TOF transient current waveforms for a 58 μm a-Se photoreceptor. (a) XTOF: $V_a = -190$ V, $t_T = 29\,\mu$sec. (b) TOF: $V_a = -350$ V, $t_T = 16\,\mu$sec.

values obtained for aluminium. There is a tendency towards saturation at high field, as is also apparent from Fig. 5.

In a few samples where τ_e did not exhibit the low-field dependence, it was possible further to investigate the field dependency. As presented in the semilogarithmic plots of τ_e against V_a in Fig. 6, over the initial range of the applied field ($E < 4 \times 10^4$ V cm^{-1}) τ_e can be expressed by

$$\tau_e = \tau_e^0 \exp\left(-\frac{\beta_{exp} E^{1/2}}{kT}\right) \quad (2)$$

where τ_e^0 is a constant obtained by extrapolation to zero field. In Table I, the values of τ_e^0, and β_{exp} for a-Se samples of different thickness are summarized. It is interesting that some of the β_{exp} values are very similar to the Poole–Frenkel coefficient given by [4]

$$\beta_{PF} = \left(\frac{q^3}{\pi\varepsilon_0\varepsilon_r}\right)^{1/2} \quad (3)$$

Taking $\varepsilon_r = 6.4$ for a-Se, β_{PF} calculated from Equation 3 is 2.96×10^{-4} eV/(V cm^{-1})$^{1/2}$.

In view of the above results, it is difficult to conclude that the electron lifetime can be deduced from the analysis of transient current signals. This is mainly because in most samples, the signal does not exhibit a single-exponential decay. It is misleading to regard τ_e^0 as the electron lifetime since the method of extrapolation which determines the zero-field value of τ_e depends on the values of τ_e at very low fields. In some samples at low fields, τ_e seems to be insensitive to field and yet in others it is field-dependent. Interpretation of the transient signal is further complicated by the presence of the spike.

From the well-defined break in transient signals, similar to those shown in Fig. 3, the electron mobility μ_e was calculated using

$$\mu = \frac{L^2}{t_T V_a} \quad (4)$$

In all samples, μ_e was found to be field-dependent. Figs 7 and 8 show log–log plots of μ_e against E for a-Se samples of various thicknesses (40 to 59 μm) and contacts (Al, Au, Cu). It can be seen that all results fall on a single line with a slope of 0.03. This indicates that the field dependence of μ_e satisfies the relation given in Equation 5. The magnitude of μ_e at a given field and the form of the field dependency are independent of the experimental method (TOF and XTOF) and contact material. The summary of drift-mobility measurements is shown in Table II. Note that the samples are prepared from pure selenium of different origins. It is apparent that μ_e is sensitive to the origin of the selenium used, due possibly to differences in their impurity contents. In Type D selenium, the impurity was so high that the electron response was dominated by trapping, and mobility could no longer be determined. The signal decayed rapidly with no apparent break. The term "trap-limited" (TLD) is used to describe this behaviour.

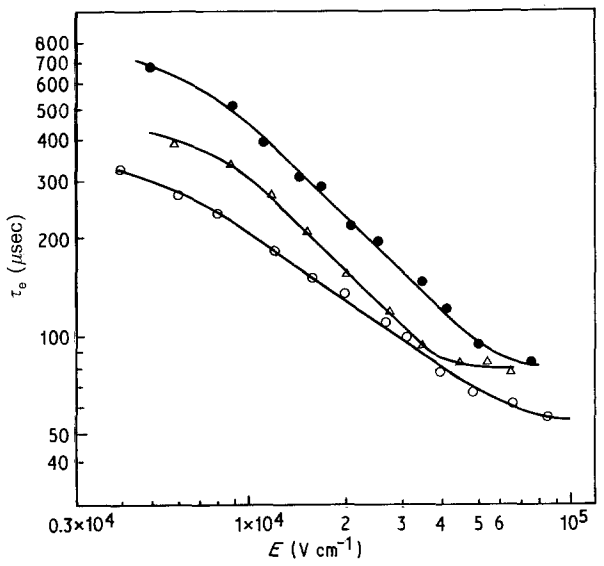

Figure 2 Log–log plot of τ_e against applied electric field for a-Se samples of various thicknesses and different substrates (results are obtained from both TOF and XTOF experiments). L = (▲) 41, (○) 49, (●) 59 μm.

2.2. Effect of impurity

The samples used for electron transport measurements were the same as those described in the previous publication in connection with hole transport [1]. In a-Se + y p.p.m. Cl and a-Se–Te + y p.p.m. Cl, there was no electron response due to the presence of electron traps generated by chlorine. Since transient signals from both XTOF and TOF experiments were similar, it is very unlikely that the observed behaviour is an experimental effect. It has also been reported by

TABLE I Electric field dependence of electron photocurrent time constant for a-Se samples of different top and bottom electrodes

Sample thickness (μm)	Top electrode	Bottom electrode	τ_e^0 (μsec)	β_{exp} (10^{-4} eV/(V cm^{-1})$^{1/2}$)
40	Al	Au	600	2.72
	Au	Au	430	3.26
58	Al	Au	330	3.03
	Al	Al	560	3.35
	Al	Cu	490	2.56

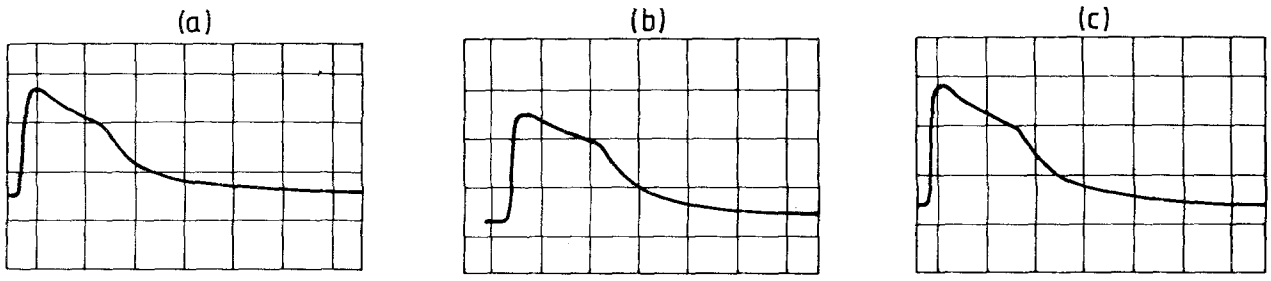

Figure 3 Effect of top contact on TOF hole current waveform in a-Se photoreceptors: (a) gold, (b) aluminium and (c) copper top contact. Aluminium substrate, $V_a = -300$ V, scale 10 μsec per division.

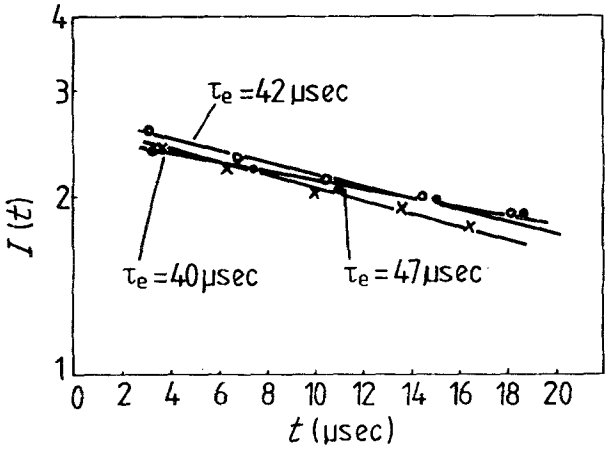

Figure 4 Semilogarithmic representation of the waveforms in Fig. 3. (x) Gold, (●) aluminium, (○) copper top contact.

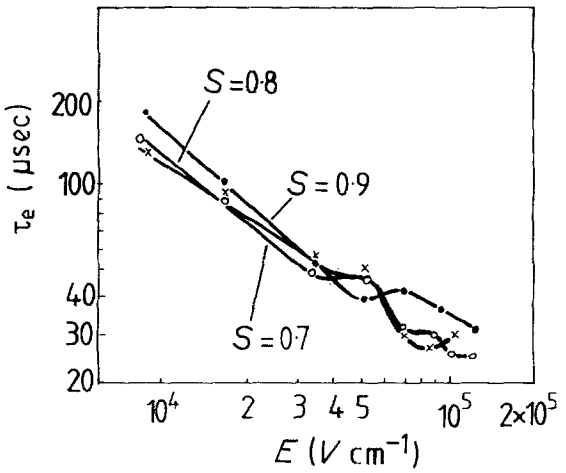

Figure 5 Log–log plot of τ_e against applied electric field E for TOF electron response in a-Se samples with different top contacts. (x) Gold, (●) aluminium, (○) copper top contact; $L = 58\,\mu$m.

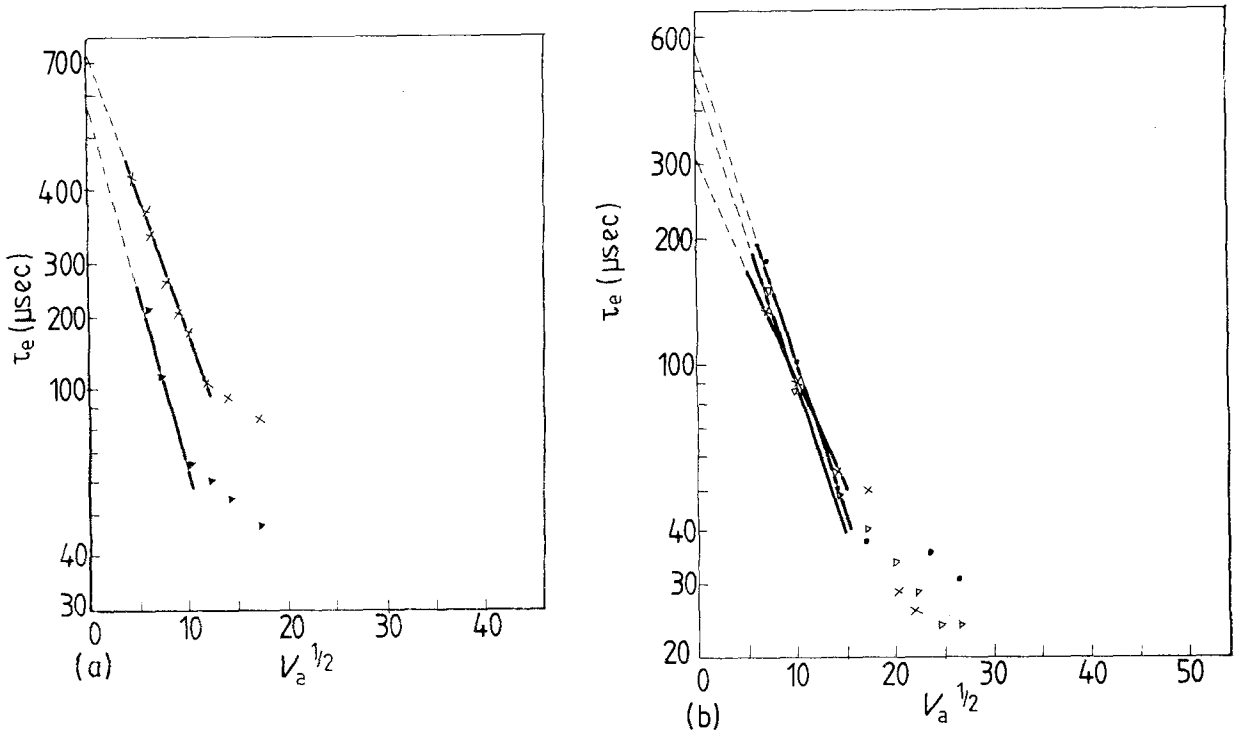

Figure 6 Logτ_e against V_a for a-Se samples of different origin: (a) common top electrodes, different substrates; (b) common substrates, different top electrodes ($L = 58\,\mu$m). (x) Al/Se/Au, (▲) Au/Se/Au, (●) Al/Se/Al, (△) Al/Se/Cu.

TABLE II Drift mobility data in samples prepared from pure selenium of different origins

Origin of selenium	μ_e ($cm^2 V^{-1} sec^{-1}$) at $E = 10^5 V cm^{-1}$	n in $\mu_e \propto E^n$
A	7.2×10^{-3}	0.04
B	7.7×10^{-3}	0.08
C	6.8×10^{-3}	0.12
D	TLD	–

other investigators that chlorine addition progressively shortens the electron range which is defined as $\mu\tau$ [5, 6]. In the rest of the system, transient signals were well defined but they had features similar to those described for electron response in pure selenium. The interpretation of the decay time constant τ_e is therefore ambiguous and it will not be discussed any further.

Fig. 9 shows that the field dependence of μ_e in various selenium-based samples satisfies

$$\mu_e \propto E^n \tag{5}$$

The values of μ_e at $E = 10^5 V cm^{-1}$ and constant n in Equation 5 are given in Table III. The following observations emerge from these results:

(a) The addition of arsenic slightly reduces μ_e but it drastically increases the field dependence. n in $\mu_e \propto E^n$ is 0.03 to 0.14 for pure selenium and it is 0.25 for Se + 0.3% As. This is due to the additional traps introduced by arsenic [7].

(b) The addition of tellurium progressively reduces μ_e and progressively increases the field dependency.

TABLE III Effect of impurity on electron mobility

Content	μ_e at $E = 10^5 V cm^{-1}$	n in $\mu_e \propto E^n$
Se + 0.3% As	3.8×10^{-3}	0.25
Se + 0.3% As + 30 p.p.m. Cl	2.8×10^{-3}	0.14
Se + y p.p.m. Cl (y = 30, 40, 60)	TLD	–
Se + 3.5% Te	1.5×10^{-3}	0.36
Se + 5% Te	1.3×10^{-3}	0.41
Se + 12% Te	3.8×10^{-4}	0.44
Se + 17% Te	3.2×10^{-4}	0.47
Se + x% Te + y p.p.m. Cl (x = 2.3, 3.7, 5.3, 12.5; y = 16, 20)	TLD	–
Se + 2.3% Te + 0.3% As + 20 p.p.m. Cl	2×10^{-3}	0.24

This is due to tellurium-induced shallow traps. The drift mobility-temperature data of the other investigators indicates that the hold transport is controlled by two sets of discrete shallow traps. The energy of the first set is 0.29 eV above the valence band edge, E_V, which is that already present in pure selenium. The second set is tellurium-induced and it is at 0.43 eV above E_V. It is the increase in concentration of these traps with tellurium content which results in a progressive reduction in μ_e.

(c) There is no electron response in samples with combinational doping of tellurium and chlorine. This can be attributed to rapid electron trapping as in

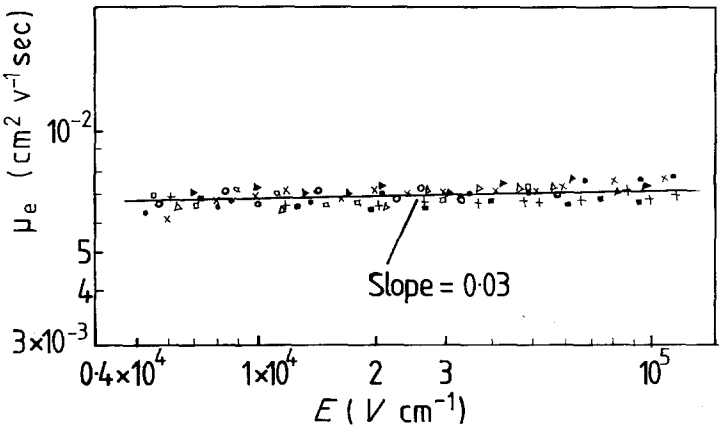

Figure 7 Log–log plot of electron drift mobility μ_e against applied electric field E for a-Se samples of various thicknesses and different substrates (results are obtained from both XTOF and TOF experiments). XTOF: (□, ○, △) Al/Se/Au; TOF: (■, ×, +) Al/Se/Au, (●, ▲) Au/Se/Au.

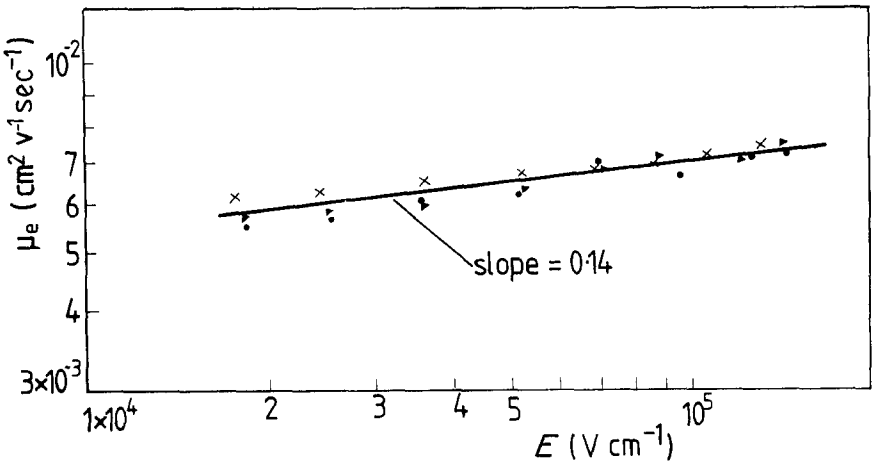

Figure 8 Log–log plot of TOF electron drift mobility μ_e against applied electric field E for a-Se samples with different top electrodes. (x) Gold, (●) aluminium, (▲) copper top contact; L = 58 μm.

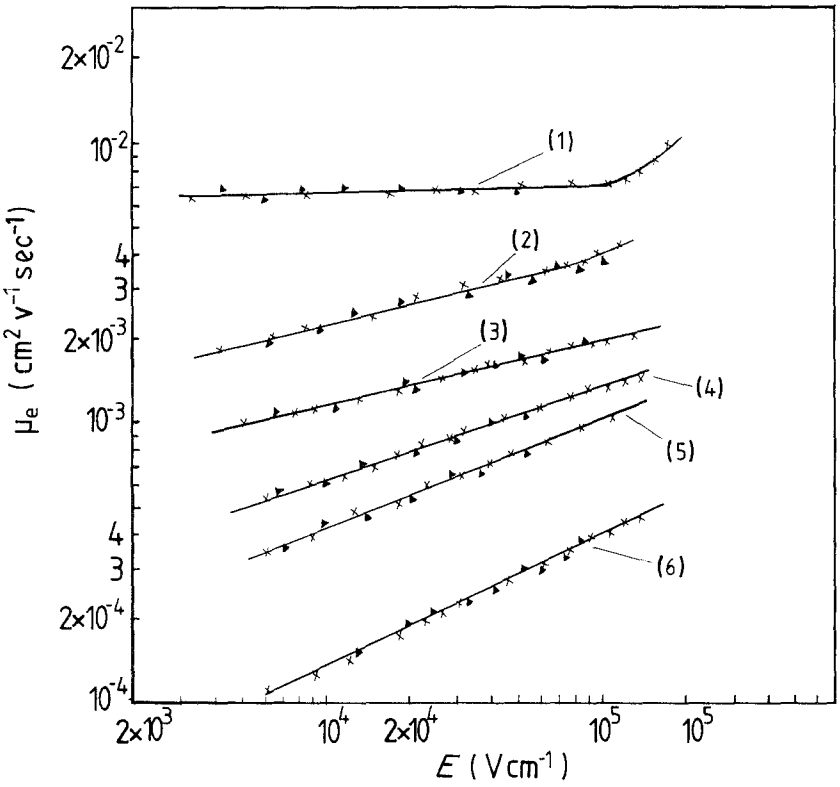

Figure 9 Electric field dependence of (▲) XTOF and (x) TOF electron drift mobility in various a-Se based systems: (1) a-Se (L = 59 μm); (2) a-Se + 0.3% As (L = 48 μm); (3) a-Se + 0.3% As + 2.3% Te + 20 p.p.m. Cl (L = 39 μm); (4) a-Se + 3.5% Te (L = 68 μm); (5) a-Se + 5% Te (L = 60 μm); (6) a-Se + 17% Te (L = 66 μm).

chlorine-doped samples or to a non-uniform field due to charge injection at the aluminium substrate.

(d) When arsenic is added to the a-Se–Te + y p.p.m. Cl system, the electron response is restored. Since it is very unlikely that the introduction of additives increases μ_e, the most plausible explanation is the destruction of chlorine-induced deep traps by arsenic. These traps may be either unbounded highly electronegative chlorine atoms or Se_3 defect centres whose concentration must be sensitive to the presence of impurities.

3. Conclusions

In order to ascertain that the electron drift mobility μ_e and electron life time τ_e are meaningful parameters characteristic of bulk transport, two different experimental techniques of XTOF and TOF were employed and transient signals under small-signal conditions were closely compared and analysed in detail. It was shown that in all systems except a-Se + Cl and a-Se–Te + Cl, electron transit times are well defined and they scale correctly with the sample thickness.

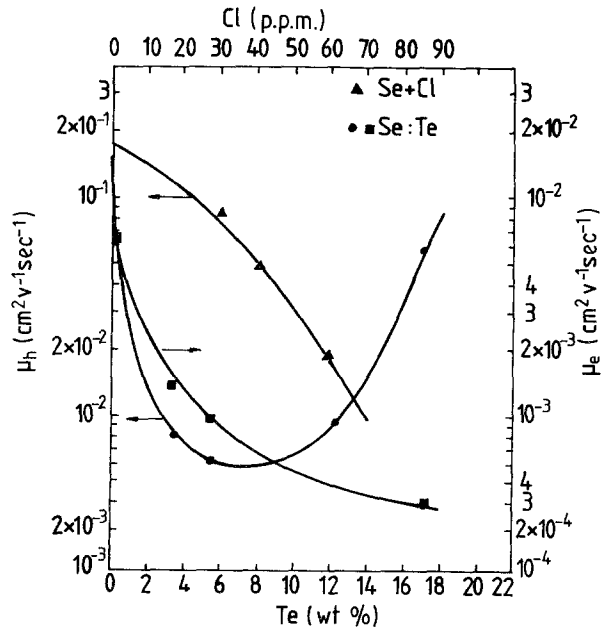

Figure 10 Effect of chlorine and tellurium on electron and hole transport properties of a-Se photoreceptors. (▼) Se + Cl; (●, ■) Se–Te.

In pure selenium, μ_e is independent of the experimental technique, sample thickness, light intensity and electrode material but it varies with the applied field in an exponential fashion. The data suggest that the transport mechanism is shallow trap-controlled [1]. Light doping of selenium with arsenic causes a reduction in the electron drift mobility. No electron response could be detected in chlorine-doped samples. The addition of tellurium in the range 0 to 20 wt % progressively decreases μ_e due to the longer residence time of the carriers at the shallow traps. In Fig. 10, the data of previous papers and the present work have been used to summarize the effect of the addition of chlorine or tellurium on both μ_e and μ_h. Electron drift mobility in all systems was found to be field-dependent of the form given by Equation 5. The consistency of μ_e–E plots among the samples of different thickness and the fact that two different experiments provide similar results suggest that the observed field dependency is a bulk property. Such a dependency has also been reported by other investigators [7, 8] and it may be attributed to the field dependence of shallow trapping [1].

Analysis of transient photocurrent signals shows that interpretation of τ_e is rather complicated. The most plausible explanation for the field dependence of τ_e in Fig. 2 is the presence of a relatively uniform distribution of positive space charge in the bulk so that

$$\tau_e = \frac{\varepsilon_0 \varepsilon_r}{\mu_e Q_0}$$

where ϱ_0 is the density of bulk space charge. The observed field dependence is due to the injection of holes into the sample from the substrate junction. It has been suggested that during evaporation a thin layer ($< 1\,\mu$m) of crystalline selenium is formed between the a-Se and aluminium substrate [9]. The field dependence arises because as the sample voltage is increased more holes are injected into the sample from the substrate junction which is of the form a-Se/γ-Se/Al. τ_e saturates at high fields due to the ample hole injection from the substrate interface to fill all the deep hole traps, i.e. $\varrho_0 = qN_d$ where N_d is the density of deep hole traps which have to be neutral when empty to give rise to the positive space charge.

References

1. S. M. VAEZI-NEJAD and C. JUHASZ, *J. Mater. Sci.* in press.
2. S. M. VAEZI-NEJAD, *Int. J. Electronics* **62** (3) (1987) 361.
3. S. M. VAEZI-NEJAD and C. JUHASZ, *Thin Solid Films* **148** (1987) 251.
4. K. TOMURA and H. MAEKAWA, *Jap. J. Appl. Phys.* **16(4)** (1977) 655.
5. M. ABKOWITZ, F. JANSEN and S. ROBINETT, *J. Vac. Sci. Tech.* **20** (1982) 875.
6. M. ABKOWITZ and F. JANSEN, *J. Non-Cryst. Solids* **59/60** (1983) 953.
7. D. M. PAI, in "Amorphous and Liquid Semiconductors", edited by J. Stuke and W. Brenig (Taylor and Francis, London, 1974) p. 355.
8. M. OKUNDA, *et al., J. Non-Cryst. Solids* **59/60** (1983) 1035.
9. E. MONTRIMAS and B. PETRITIS, *ibid.* **15** (1974) 96.

Received 29 October 1987
and accepted 25 February 1988